Potential changes in larval dispersal and alongshore connectivity on the central Chilean coast due to an altered wind climate

C. M. Aiken,[1,2] S. A. Navarrete,[1,2] and J. L. Pelegrí[2,3]

Received 6 April 2011; revised 17 September 2011; accepted 22 September 2011; published 10 December 2011.

[1] Climate change is likely to result in significant alterations in the atmospheric and oceanic circulation, which may, as a result, affect species that depend on an ocean-driven nutrient supply and particularly those that possess a dispersal phase in their life history. In this paper we investigate the potential changes in larval dispersal and connectivity of marine populations on the Chilean coast due to altered wind forcing consistent with a future climate change scenario. Numerical ocean simulations forced by modeled present-day and future winds under the Intergovernmental Panel on Climate Change A2 scenario are used to investigate the potential changes in nearshore circulation. Off-line particle-tracking simulations are then analyzed to determine resulting changes in larval dispersal and connectivity under each scenario as a function of pelagic larval duration and for two different possible larval behaviors: passive and vertical migration. It is found that the projected future winds drive an intensification of the upwelling circulation, which results in a relative annual mean surface cooling of 1°C over much of the domain, an increase in the strength of the poleward undercurrent, and a more energetic mesoscale eddy field. Neutrally buoyant larvae are inferred to have low rates of settlement under present conditions and are more strongly disadvantaged under the simulated future conditions than larvae with vertically migrating behavior. Larvae that posses an ability to sink out of the surface Ekman layer are found to have higher rates of settlement under present conditions and are, in fact, favored slightly in the A2 scenario for pelagic larval durations longer than 2 days. This behavior-dependent response to future conditions may potentially drive a reorganization of coastal communities.

Citation: Aiken, C. M., S. A. Navarrete, and J. L. Pelegrí (2011), Potential changes in larval dispersal and alongshore connectivity on the central Chilean coast due to an altered wind climate, *J. Geophys. Res.*, *116*, G04026, doi:10.1029/2011JG001731.

1. Introduction

[2] The persistent upwelling favorable wind conditions found on the central Chilean coast render it one of the most biologically productive regions of the global ocean [*Longhurst*, 1998; *Cury et al.*, 1998]. In addition to its vital role in driving fertilization of the euphotic zone, the character of the local ocean circulation is of great importance in the population dynamics of the communities of organisms that inhabit the region [*Navarrete et al.*, 2005]. Many fish and marine invertebrates possess a pelagic larval phase during which their fate is strongly affected by the coastal ocean circulation. In many cases, the pelagic larval phase is the main or only means by which geographically separated populations are connected, allowing maintenance of genetic continuity within species and metapopulation robustness through export of competent larvae to otherwise unsustainable populations. Thus the nature of the coastal circulation is intrinsically linked to the ecology of coastal marine populations.

[3] The ongoing effort to understand the ocean's role in the ecology of marine populations has uncovered a range of possible mechanisms by which competent larvae can return to shore [*Shanks*, 1995; *Largier*, 2003; *Narváez et al.*, 2006; *Queiroga et al.*, 2007]. Along eastern boundaries characterized by active and often year-round offshore Ekman transport at the surface, such as is the case for central Chile, retention times for coastal waters are short and the ability of larvae to return to shore may be dependent upon their ability to sink below the surface Ekman layer and to the existence of mesoscale or submesoscale features that produce cross-shore transport or retention close to the coast. Thus it is conceivable that, together with the expected increased in sea surface temperature and ocean acidification and their effects on larval development, changes in the character or frequency of larval transport mechanisms in the future could bring consequences for coastal invertebrate communities [*Lett et al.*, 2010; *Brochier et al.*, 2010].

[1] Estación Costera de Investigaciones Marinas, Pontificia Universidad Católica de Chile, Santiago, Chile.
[2] Laboratorio Internacional en Cambio Global, UC-CSIC, Departamento de Ecología, Facultad de Ciencias Biológicas, PUC, Santiago, Chile.
[3] Departament d'Oceanografía Física, Institut de Ciències del Mar, CMIMA, CSIC, Barcelona, Spain.

0148-0227/11/2011JG001731

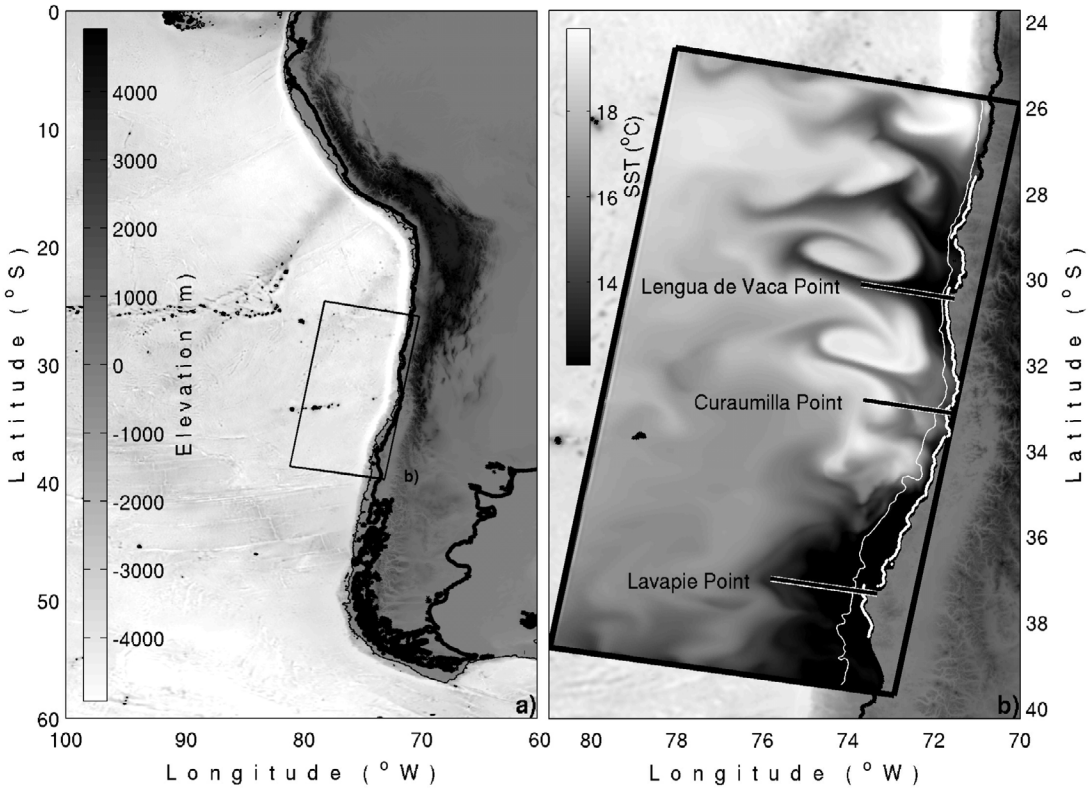

Figure 1. (left) Topography of the southeast Pacific with the boundary of the model domain indicated. The 1000 m isobath is marked. (right) Model domain with snapshot of modeled sea surface temperature (SST) from day 360 of the baseline (BL) simulation. Locations of particle release for the particle-tracking experiments are indicated in white. The 1000 m isobath is marked in white.

[4] Observations and modeling studies suggest that significant changes are occurring in the atmospheric circulation in eastern boundary systems related to increased atmospheric greenhouse gas concentrations [*Bakun*, 1990; *Mendelssohn and Schwing*, 2002; *Echevin et al.*, 2011]. A poleward shift and intensification of the southerly winds that prevail along much of the coast is a robust result from the Coupled Model Intercomparison Project (CMIP3), used as part of the Intergovernmental Panel on Climate Change (IPCC) Fourth Assessment Report (AR4) [*Garreaud and Falvey*, 2008; *Sen Gupta et al.*, 2009; *Echevin et al.*, 2011]. As first suggested by *Bakun* [1990] and supported in a number of recent observational studies [*García-Reyes and Largier*, 2010; *Gutiérrez et al.*, 2011], this altered atmospheric circulation is expected to result in an intensification of coastal upwelling in the midlatitude eastern boundary systems. Thus the character of the coastal circulation, and consequently of the dispersal of coastally released larvae, may experience significant changes over the course of the present century. However, as upwelling is not a two-dimensional phenomenon, changes in its intensity will not bear a simple dependence on changes in sea surface wind and vertical stratification but will also vary as a response to changes of the coastal circulation patterns. Thus, it is not evident how the dispersal of coastally released larvae may change over the course of the present century.

[5] The study sets out to test the hypothesis that a future altered wind climate will result in significant changes in patterns of connectivity of marine organisms inhabiting the central Chilean coast. In order to investigate the potential changes in the coastal circulation in central Chile and their effect upon marine ecosystems, numerical simulations were performed under both present-day and future climate scenarios using hydrodynamic and larval transport models. We show that future wind forcing is likely to drive an intensified upwelling circulation whose impact upon coastal invertebrate communities is sensitive to a larval swimming behavior that varies the position in the water column. Following an introduction and description of the models in sections 1 and 2, respectively, the methods are discussed in section 3, and results of these simulations are presented in section 4 and discussed in section 5. Concluding remarks are made in section 6.

2. Site Description

[6] The study deals with the section of the central Chilean coast located between 26°S and 39°S (Figure 1). An excellent overview of the atmospheric and oceanic circulation on South America's Pacific coast is provided by *Strub et al.* [1998]. The Chilean coastline has a predominantly meridional orientation and a shelf that is extremely narrow, especially toward the north. The Andes mountain range forms a continuous barrier that intersects the atmospheric marine boundary layer and supports the propagation of topographically trapped disturbances. The atmospheric circulation in this region is dominated by the south eastern Pacific

Subtropical Anticyclone, which drives equatorward winds along the coast. The summer intensification of the southerly winds becomes more prominent with increasing latitude. As a result, wind-driven upwelling is confined to summer in southern Chile but occurs year round in northern Chile.

[7] The understanding of the oceanic circulation continues to be limited by the paucity of observational data in the south east Pacific, but nonetheless the existence of a banded velocity field composed of a series of alongshore currents of alternating direction has been inferred [*Strub et al.*, 1995; *Shaffer et al.*, 1999]. The equatorward Chile Coastal Current is a shallow coastal jet that develops adjacent to the coast during periods of southerly winds [*Aiken et al.*, 2008]. Beneath the Chile Coastal Current, the poleward Peru Undercurrent follows the shelf break and may extend from depths of 50–500 m, with a core that sinks from 150 m depth in the north to in excess of 300 m in the south. The Peru Undercurrent is typically of the order of 10 cm s^{-1} but has been observed to exceed 50 cm s^{-1} and to occasionally extend to the surface [*Johnson et al.*, 1980; *Atkinson et al.*, 2002]. Farthest offshore is found the broad sluggish Peru Current (also known as the Humboldt Current), the eastern boundary current of the south Pacific. Observations also suggest the existence of the poleward Peru-Chile Counter Current running between the Chile Coastal Current and Peru Current at the surface, and an offshore branch of the Chile Coastal Current.

[8] The nearshore velocity field is also characterized by a relatively high level of mesoscale variability in the form of eddies and filaments [*Djurfeldt*, 1989; *Cáceres*, 1992; *Batteen et al.*, 1995; *Leth and Shaffer*, 2001; *Hormazabal et al.*, 2004]. These structures are generated through baroclinic instability following coastal upwelling of relatively dense water [*Leth and Middleton*, 2004]. Although upwelling-favorable winds and offshore Ekman transport occur throughout central Chile, the most intense upwelling is associated with major geographical features, such as the Lengua de Vaca (30°S), Curaumilla (33°S) and Lavapie (37°S) points [*Johnson et al.*, 1980; *Strub et al.*, 1998; *Figueroa and Moffat*, 2000; *Aiken et al.*, 2008].

[9] The upwelling driven at Lavapie Point has received particular interest because the waters nearby produce up to 4% of the annual global fish catch [*Mesias et al.*, 2001; *Leth and Shaffer*, 2001; *Mesias et al.*, 2003; *Leth and Middleton*, 2004].

3. Methods

3.1. Hydrodynamic Model

[10] Simulations of the ocean circulation on the central Chilean coast were performed using the Regional Ocean Modeling System (ROMS), a hydrostatic split-explicit primitive equation ocean model that has found extremely wide use for regional circulation studies. Details of the numerics of ROMS are given by *Shchepetkin and McWilliams* [2005]. ROMS has proven to be capable of reproducing a realistic circulation in each of the eastern boundary current systems [*Marchesiello et al.*, 2003; *Marchesiello and Estrade*, 2007; *Estrade et al.*, 2008; *Capet et al.*, 2008; *Mason et al.*, 2010].

[11] The model domain encompasses the section of the Chilean coast between approximately 39°S and 26°S, and extends approximately 750 km offshore (Figure 1). An orthogonal grid is used, rotated by approximately 10° clockwise to follow the general trend of the coast. Horizontal resolution is approximately 3 km alongshore, but in the cross-shore direction increases smoothly from 6 km at the open western boundary to approximately 1.5 km over the 100 km closest to the coast. The coastal increase in resolution allowed an improved representation of the coastal boundary layer and of the Chile Coastal Current, features that assume increased importance for determining the fate of coastally released particles [*Largier*, 2003; *Aiken et al.*, 2007]. This resolution also is sufficient to resolve well the instability processes that are responsible for much of the variability in upwelling regions [*Capet et al.*, 2008]. Bathymetry was interpolated from the ETOPO2v2 [*NOAA*, 2006], while the land mask was determined from world vector shoreline (http://shoreline.noaa.gov/data/datasheets/wvs.html). Following standard practice to limit the pressure gradient errors that occur over steep terrain in sigma coordinate models such as ROMS, a local Hanning filter was applied recursively to the bathymetry so as to remove slopes that exceed the criteria $\Delta h/2\ h > 0.2$, where h is the water depth [*Haidvogel and Beckmann*, 1999]. Although parts of the Chilean trench exceed 7000 m in depth, a maximum depth of 4000 m was imposed, and all seamounts were removed. The radiation/nudging open boundary conditions of *Marchesiello et al.* [2003] were applied to temperature, salinity, and all components of velocity, at the three open boundaries, with inward (outward) relaxation time scales of 1 day (360 days). The seasonally varying values for temperature and salinity applied at the open boundaries were taken from the NODC Ocean Data Atlas [*Locarnini et al.*, 2006] (above 1500 m) and the Levitus data set *Antonov et al.* [1998] (below 1500 m), while geostrophic velocities relative to 4000 m determined from the temperature and salinity data supplied the open boundary velocity field. The velocity field so determined captures some of the main features of the coastal circulation, including a surface intensified coastal jet, a poleward undercurrent at the shelf break consistent with observations, and broad northwestward flow farther offshore [*Strub et al.*, 1998]. Zero gradient conditions were applied to surface elevation at the open boundaries. Nudging layers were employed in the 150 km prior to each open boundary, in which salinity, temperature and surface elevation were nudged toward their climatological values. The nudging time scale increased smoothly a value of 360 days next to each open boundary toward infinity in the domain interior. Similarly, 150 km wide sponge layers were applied to the momentum field, wherein eddy viscosity (diffusivity) decreased smoothly toward the internal value of zero from a value of 100 $m^2\ s^{-1}$ (50 $m^2\ s^{-1}$) next to each open boundary. These values are typical for regional ocean models [e.g., *Marchesiello et al.*, 2001].

[12] Climatological heat and salt fluxes were calculated from the NCEP reanalysis [*Kistler et al.*, 2001]. Relaxation toward climatological sea surface temperature was included in the form of a temperature-dependent heat flux correction term, while surface salinity was also relaxed toward climatology. Surface momentum fluxes were derived from the model of *Garreaud and Falvey* [2008] (hereafter referred to as GF). GF configured the PRECIS atmospheric circulation model [*Jones et al.*, 2004] for the Chilean region of the south east Pacific. They performed simulations for the period

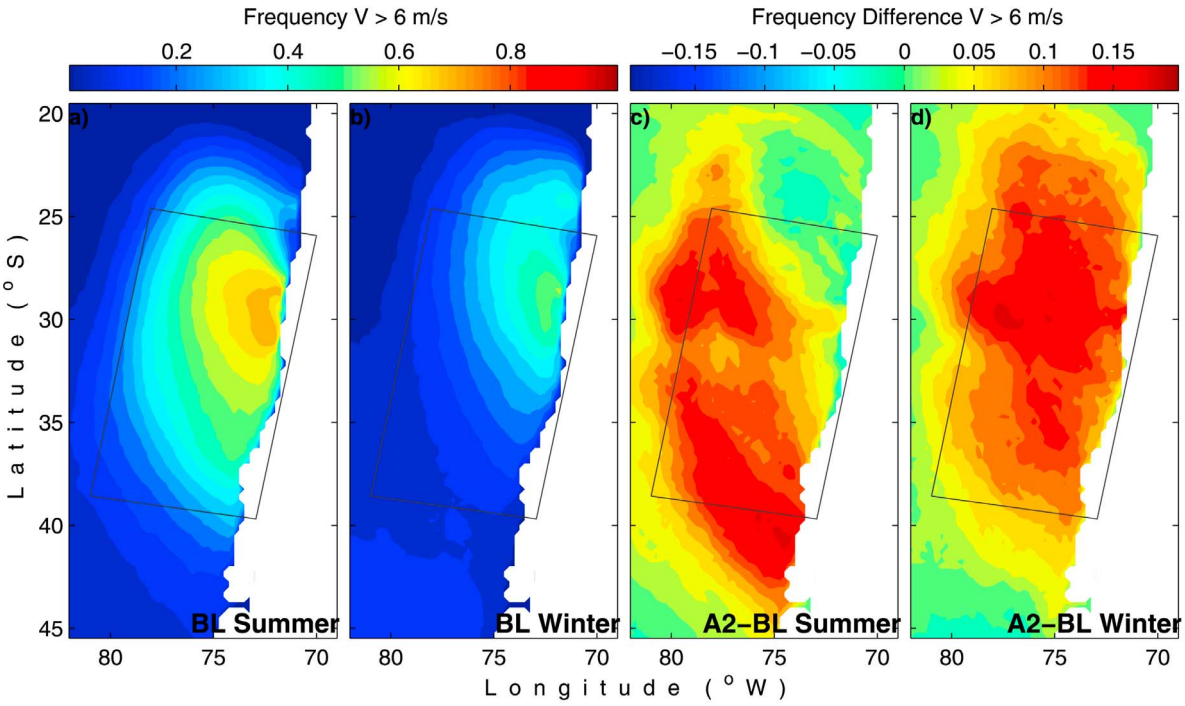

Figure 2. (left) Frequency (in events per day) of upwelling favorable winds, as defined by southerly winds >6 m s^{-1}, during summer and winter from the BL simulation and (right) difference in frequency between the BL and A2 simulations.

1960–1990 under observed forcing, hereafter referred to as the baseline (BL) scenario, and 2070–2100 under the A2 climate change scenario. Lateral boundary conditions for the GF model were taken from the 20C and A2 integrations of the Hadley Centre Atmospheric Model (HadAM3), an atmospheric GCM found to simulate well the large-scale atmospheric circulation of the west coast of South America [*Fuenzalida et al.*, 2007]. Surface heat fluxes were derived from the HadISST1 data set [*Rayner et al.*, 2003]. GF demonstrate that the integration simulating present-day conditions is in close agreement with Quikscat observations. Because of the relatively high resolution of 25 km and the availability of daily averaged data, the PRECIS wind field resolves well variability in the southerly jet, the principal driver of upwelling/relaxation on the central Chilean coast [*Muñoz and Garreaud*, 2005].

[13] A predominant feature of the PRECIS simulations demonstrated by GF is the poleward shift and intensification of the upwelling favorable southerly wind regime that occurs under the A2 emissions scenario (see Figure 2 and GF's Figure 2). This is also a robust result from the GCM simulations performed for the Fourth Assessment Report (AR4) of the Intergovernmental Panel on Climate Change (IPCC) under a range of increased radiative forcing scenarios [*Sen Gupta et al.*, 2009]. This robust change in the wind field is driven by an intensification of the zonal atmospheric pressure gradient resulting from increased radiative forcing. In order to simplify the analysis and concentrate on the role of the altered wind conditions, fluxes of heat and freshwater were identical for both simulations. That is, the differences between the two runs can be unambiguously attributed to the differences in the applied wind fields alone, and do not include any direct influence from ocean warming or external variability such as ENSO or coastally trapped waves. No consistent trend for the atmosphere–ocean heat flux is present in the IPCC CMIP3 simulations for this region, and a multimodel mean shows it to be close to present-day conditions [*Sen Gupta et al.*, 2009]. Direct effects of surface heating upon the ocean momentum field are likely to be of secondary importance in any case. In the following, in addition to annual mean fields we present means over the periods October–March and April–September, for convenience referred to as summer and winter, respectively. The summer period corresponds to the months typically associated with upwelling in central Chile.

3.2. Particle-Tracking Model

[14] Simulations of larval dispersal were performed using the off-line particle-tracking package ARIANE [*Blanke and Raynaud*, 1997]. ARIANE employs an innovative algorithm in which the particle trajectories are determined by calculation of the exact three-dimensional stream function at each time instance for which the velocity field is available. The algorithm is efficient and accurate provided that the frequency with which the hydrodynamic model output is recorded is sufficient to resolve the evolution of the velocity field. The velocity field from the hydrodynamic model was recorded every 12 model hours, a frequency chosen to be as long as possible to minimize storage overhead but without compromising accuracy in the particle tracking. A test performed using a velocity field write frequency of 6 h agreed closely with the results when a 12 h write frequency was used. Thus, the results presented below are relatively insensitive to increased temporal resolution of the velocity field.

[15] An ensemble of particle-tracking simulations were performed, involving the daily release of a patch of "larvae" from a series of 400 evenly spaced locations separated by 3 km in the alongshore direction (Figure 1). Each patch was composed of nine particles spread evenly within the nearest model cell, and located initially at the surface. Patches were released synchronously once every model day at 00:00. Given that the wind field is composed of daily averages, the once daily release time does not alias subdaily variability such as would be associated with the sea breeze. The particles were integrated forward in time for 90 days and their position recorded once per day. Larvae develop competency to settle over a period of time known as the pelagic larval duration. While the pelagic larval duration will typically be sensitive to temperature, with warmer conditions accelerating development, here we assume that this timescale is independent of temperature. The consequences of this assumption are discussed below. A "larva" was considered to have "settled" on the coast at a given pelagic larval duration if it was located within 2 grid cells of the coast (approximately 3 km) after that lapse of time. Clearly the criteria used here for larvae to settle is much weaker than that which occurs in nature, where larvae must cross the coastal boundary layer and encounter a suitable substrate within their competency time window [*Shanks et al.*, 2010]. In addition, we do not consider larval mortality (e.g., because of starvation or predation), which can be extremely high and may show a complex dependence upon the local properties of the ocean [*Morgan*, 1995; *Vargas et al.*, 2006; *Chiu et al.*, 2008]. Thus, the only form of larval loss in the model corresponds to "larval waste", i.e., larvae that are found too far from appropriate settling habitat by the end of the competency period. Nonetheless, the spatiotemporal patterns of "settlement" are expected to reflect that which occurs in nature for larvae with broadly similar attributes (pelagic larval duration, vertical swimming), and hence serve as a diagnostic of possible relative changes in larval dispersal due to an altered wind climate. Because many processes that control the transport of larvae across the coastal boundary layer are not included in the model, such as waves, tides or the sea breeze, and the boundary layer itself is underresolved, applying a stricter criteria would not add greater realism to the settlement statistics.

[16] Identical ensembles of simulations were performed for two distinct vertical swimming behaviors: (1) passive dispersal as a neutrally buoyant particle and (2) a diel vertical migration to 50 m, hereafter referred to as neutrally buoyant and vertically migrating larvae, respectively. In the former the water column depth is determined by integration of the vertical velocity, while in the latter the vertical position of each particle was enforced to be $50 \sin(2\pi t)$ m, where t is the elapsed time in days. While the real larval swimming behaviors are potentially much more complex than either of these scenarios, several studies have shown that assuming simple larval behaviors in realistic but simple hydrodynamic models can reproduce some features of the spatial structure of benthic populations [*Gilg and Hilbish*, 2000; *Hohenlohe*, 2004; *Galindo et al.*, 2006; *Cowen et al.*, 2006]. In addition, the actual swimming behaviors of the benthic species that inhabit the central coast of Chile are largely unknown. Here we consider two simplified possibilities to illustrate the potential for larval swimming behavior to influence patterns of connectivity and their response to future ocean conditions.

[17] The results of the larval dispersal simulations were summarized through the determination of connectivity matrices as a function of pelagic larval duration, season and year from the model settlement data. The value of the connectivity matrix $C_t(i, j)$ is given by the fraction of particles released from location i that settle at location j after pelagic larval duration t. Therefore each row of C_t gives the probability P_S of settlement at the corresponding location as a function of release location, and each column the probability P_R of successful release as a function of settlement location. P_R is commonly referred to as the dispersal kernel. We note that the calculated connectivity matrix does not take into account many factors that influence net fluxes of larvae between populations, such as spatial variations in larval production rates, larval mortality, and temperature-dependent pelagic larval duration. The connectivity matrices summarize the component due to oceanic transport only.

4. Results

4.1. BL Circulation

[18] The simulated circulation under baseline wind forcing reproduces well the principal observed features of the system. Seasonally and alongshore averaged offshore transects of temperature and velocity are shown in Figure 3. A northward current consistent with the equatorward Peru Current is evident approximately 100–200 km from the coast. Maximum equatorward flow associated with the Peru Current of approximately 10 cm s^{-1} occurred during summer. A Peru Undercurrent was produced next to the coast and over the shelf break along the length of the domain. Consistent with observations [*Hormazábal*, 1995], the zone of poleward velocity commonly reached to the surface, and the subsurface velocity maximum of up to 30 cm s^{-1} was generally located around 150 m depth. In the alongshore average the Peru Undercurrent was slightly stronger and shallower in summer, but this tendency decreased with increasing latitude. A relatively shallow coastal jet, consistent with the Chile Coastal Current, was most commonly found in the south of the domain during summer, but was only intermittently present along the coast elsewhere on the coast. The mean cross-shore velocity is that of a classic coastal upwelling cell, with offshore transport in the shallow surface Ekman layer and more sluggish onshore flow below. The strength of the offshore flow decreased in winter together with the decrease in southerly winds.

[19] The model was also able to reproduce the dominant mesoscale structures associated with upwelling regions, in the form of eddies and filaments (e.g., Figure 1b). The simulation mean surface eddy kinetic energy (Figure 4) was low immediately next to the coast and reached maximum intensity offshore, consistent with the work by *Capet et al.* [2008].

4.2. A2 Circulation

[20] Relative to BL, the A2 wind field has stronger southerlies that extend farther south and occur over a greater fraction of the year. In addition, the periods of strong southerlies associated with intense coastal upwelling (defined here by daily mean northward velocities exceeding 6 m s^{-1}, following GF) become more frequent (Figure 2). Given the relationship between coastal upwelling and strong southerlies it is not surprising that the response of the ocean model to

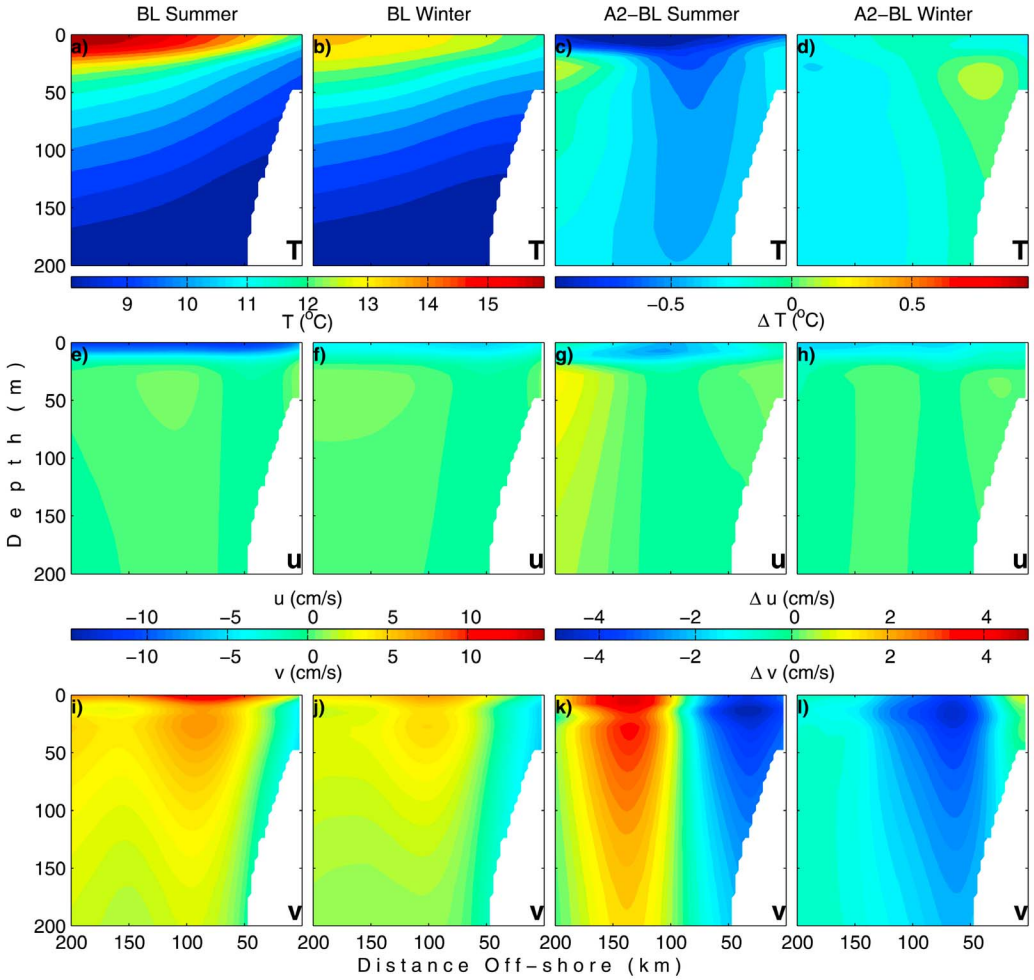

Figure 3. Offshore transects of temperature (T) and cross-shore (u) and alongshore velocity (v) averaged in the alongshore direction and over the indicated season. (a, b, e, f, i, j) Transects averaged over the BL simulation and (c, d, g, h, k, l) the averaged difference between the A2 and BL simulations. Positive (u, v) velocities are in the onshore and equatorward directions, respectively.

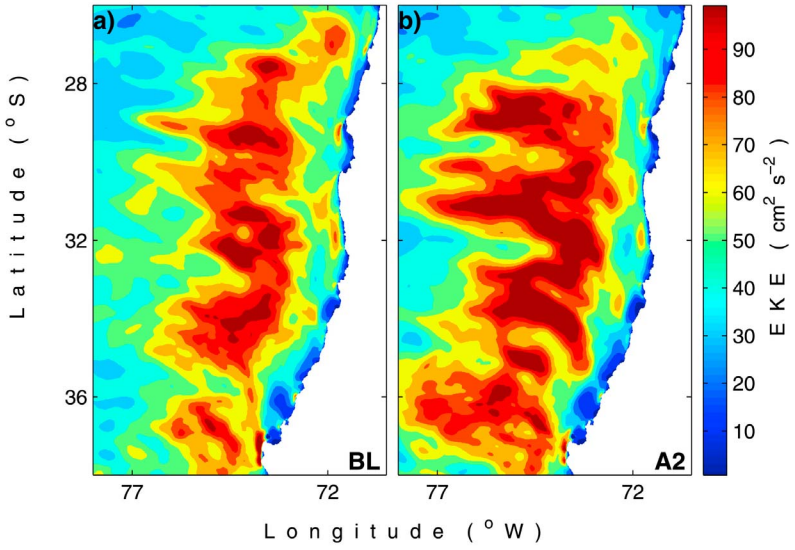

Figure 4. Surface eddy kinetic energy averaged over (a) the BL and (b) A2 simulations.

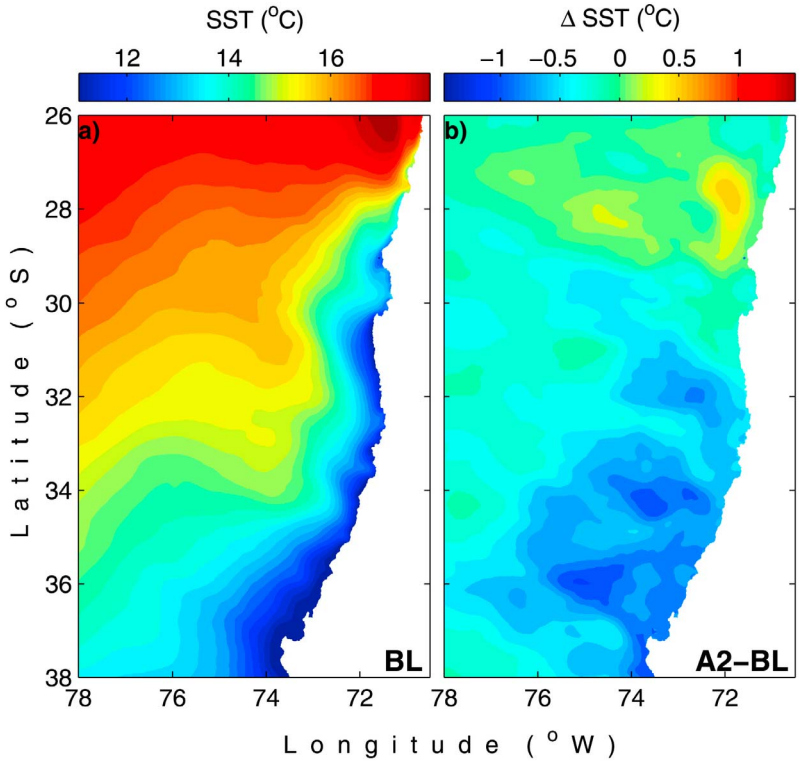

Figure 5. (a) Annual mean SST from the BL simulation and (b) SST difference between A2 and BL simulations.

A2 forcing is to produce increased upwelling relative to BL. The intensification of the coastal upwelling circulation under A2 winds may be appreciated in Figure 3. In both seasons, but principally in summer, the offshore velocity in the surface Ekman layer, the onshore flow beneath, and the coastal jet are each significantly stronger in A2 than in BL. In consequence, southward of 30°S, the mean the annual mean sea surface temperature (SST) in the A2 simulation is on average 1°C lower than in BL (Figure 5). The zone of relative surface cooling corresponds to the location of greatest increase in the frequency of upwelling favorable wind events (Figure 2). The slight increase in SST northward of 30°S, is associated with an intensification in the strength of the Peru Undercurrent which, at these latitudes, extends to the surface and brings slightly warmer water from the north. It may be noted that, while an increase in the upwelling circulation occurred in both summer and winter, a corresponding large change in SST only occurred in summer, a result of the much weaker vertical temperature gradients in winter. As discussed in GF, a relative reduction in SST is likely to have consequences for the local climate. A significant increase in eddy kinetic energy occurred in the A2 run relative to BL, driven by the increased upwelling intensity and hence baroclinicity of the water column (Figure 4b).

4.3. BL Connectivity

[21] Figure 6 illustrates the connectivity matrices for the two contrasting larval swimming behaviors averaged over the entire BL simulation for pelagic larval duration of 2, 15 and 60 days, which encompass the pelagic larval duration times of many common invertebrate species [*O'Connor et al.*, 2007]. The connectivity patterns can be seen to differ significantly between the two swimming behaviors. While, as expected, significant self-recruitment occurs in each case, the mean displacement of settlers is generally much smaller for neutrally buoyant than vertically migrating larvae. In both cases the mean displacement of successful settlers is southward, but that of unsuccessful neutrally buoyant larvae is northward. This indicates that neutrally buoyant larvae that return to shore experience a distinct advective environment to those lost as larval waste [*Largier*, 2003; *Aiken et al.*, 2007]. In addition, vertically migrating larvae have a much higher rate of settlement than those with no swimming ability, especially at longer pelagic larval durations, suggesting that this swimming mechanism may result in a significant reduction in larval waste. The large difference in settlement success rate between the two swimming behaviors can be more clearly seen in the time mean P_R, plotted in Figure 7a for a pelagic larval duration of 30 days as a function of release location along the coast. Figure 7a also reveals a marked tendency for P_R to decrease toward the north for neutrally buoyant larvae, and increase toward the north for vertically migrating larvae.

[22] The dependence of settlement and connectivity upon pelagic larval duration may be seen in Figure 8, in which the average settlement rate at each release location is plotted as a function of the month of year in which the larvae were released. Whereas neutrally buoyant larvae have very low

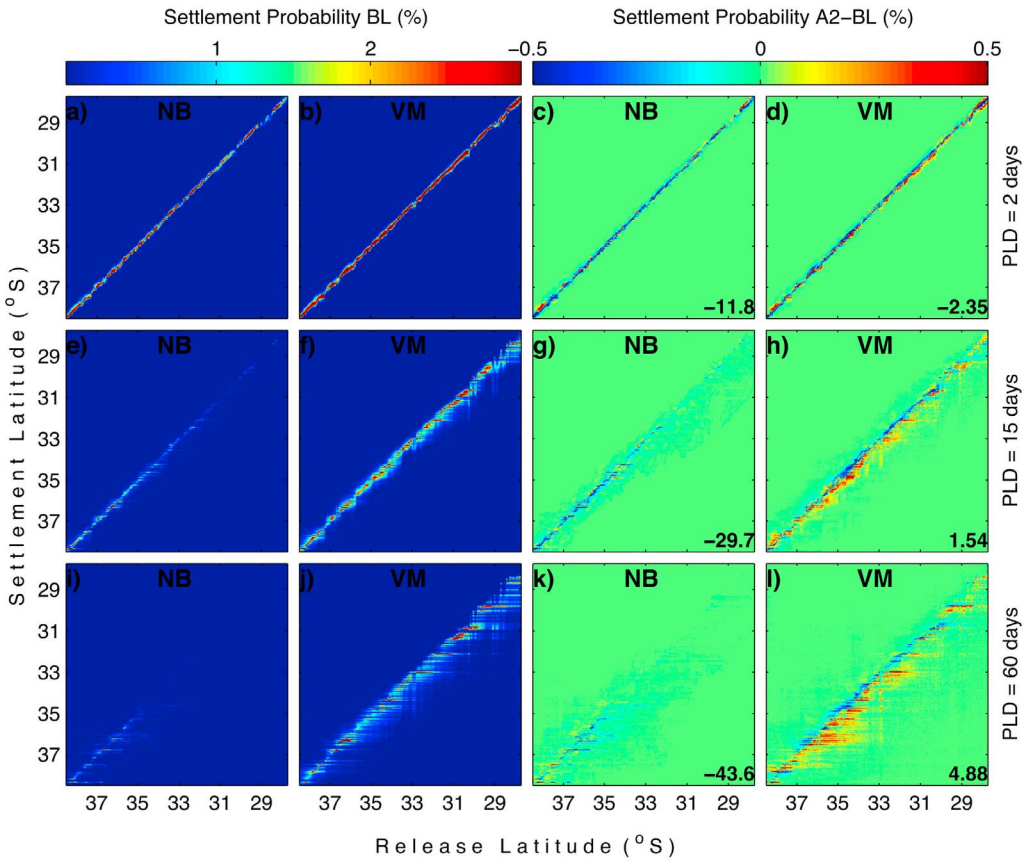

Figure 6. (a, b, e, f, i, j) Connectivity matrices for neutrally buoyant (NB) and vertically migrating (VM) larvae and planktonic larval durations of 2, 15, and 60 days from the BL simulation. (c, d, g, h, k, l) The difference to the corresponding connectivity matrices from the A2 simulation. The number in the bottom right-hand corner gives the percentage change in total settlement between the A2 and BL simulations.

probabilities of settling for pelagic larval durations >2 days, especially for the northern section of the domain, vertically migrating larvae maintained high settlement probability at most locations, even for a pelagic larval duration as long as 60 days. At a pelagic larval duration of 2 days the probability of settling is relatively uniform at all locations for both swimming behaviors, but as pelagic larval duration increases substantial spatial variability in settlement success rate was apparent, even between adjacent locations. Nonetheless, some regional patterns exist. For neutrally buoyant larvae there is a strong trend for the settlement rate to decrease with distance north, with very little settlement occurring north of 32°S for a pelagic larval duration greater than 2 days. In contrast, settlement of vertically migrating larvae released from most locations is possible throughout the region out to a pelagic larval durations of 90 days.

[23] Figure 8 also reveals strong but differing seasonality in settlement for both types of swimming behavior and at all pelagic larval durations. For neutrally buoyant larvae, settlement is almost completely confined to winter at all pelagic larval durations. Vertical migrators with short pelagic larval durations also tend to experience greatest success in winter but, for pelagic larval durations longer than a few days, there exists a tendency for increased settlement to occur in summer, especially southward of 34°S.

4.4. A2 Connectivity

[24] The connectivity matrices determined from the A2 simulation are qualitatively very similar to those for BL, with the following differences. First, there was a general decrease in the probability of successful settlement of neutrally buoyant larvae under the future scenario, which reached almost 30% at a pelagic larval duration of 15 days and over 40% reduction at a pelagic larval duration of 60 days (Figure 6). In contrast, settlement of vertically migrating larvae was slightly (<5%) but positively affected by the altered ocean conditions at pelagic larval durations of over 2 days. Second, there was a trend for vertically migrating larvae to settle increasingly southward under the altered ocean conditions, especially so south of about 33°S (Figure 7d), but no consistent change in settlement direction from the origin was observed in neutrally buoyant larvae (Figure 6). Third, the alongshore pattern of changes in settlement under altered ocean conditions was not uniform. In particular for neutrally buoyant larvae, the reduction in settlement was more pronounced in the southern portion of the domain (Figure 7d), largely because settlement in the northern section was already extremely low.

[25] The spatial distribution of the change in settlement rate is more clearly shown in Figure 8b. The largest reductions in neutrally buoyant settlement occur south of 32°S.

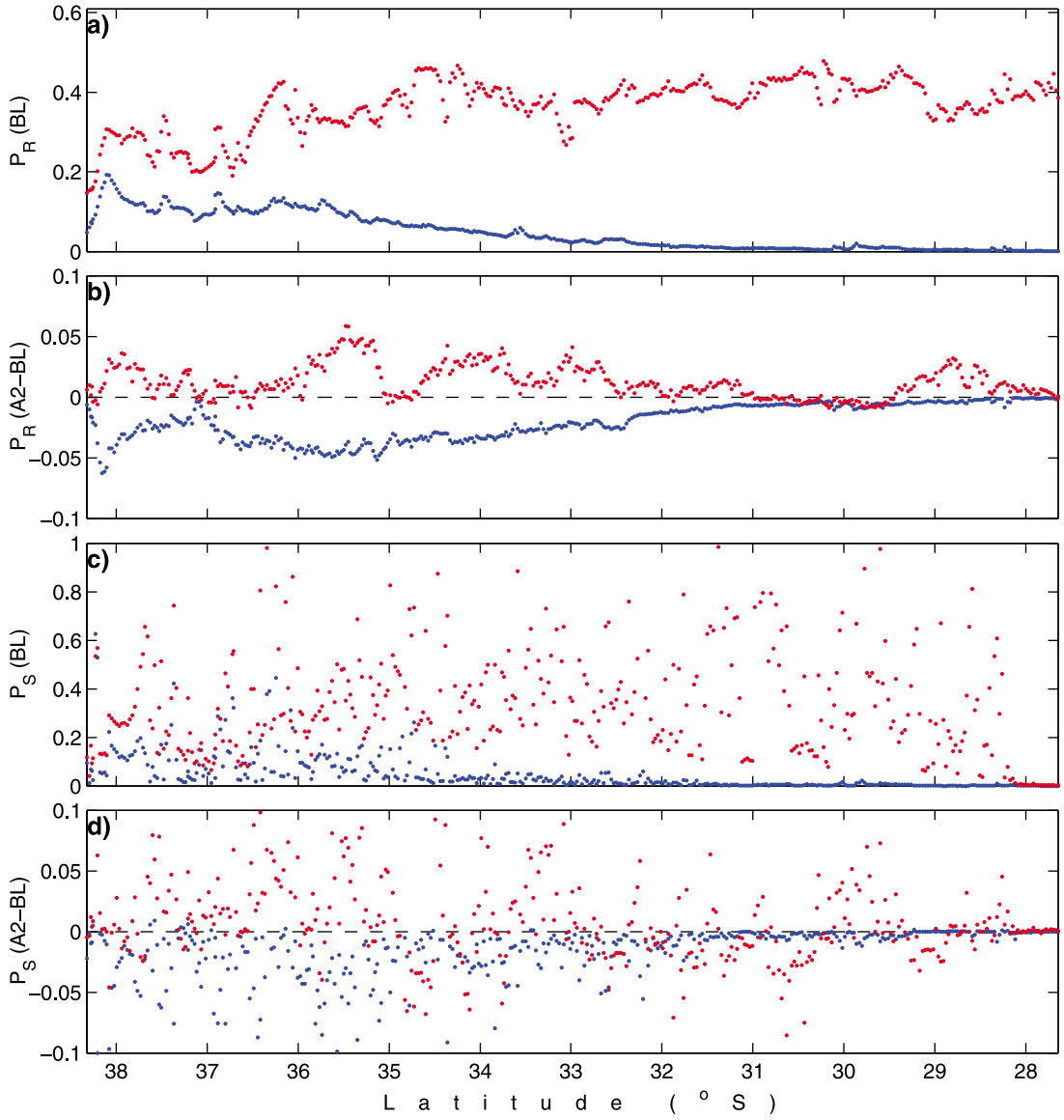

Figure 7. (a) Probability of settlement of neutrally buoyant (blue) and vertically migrating (red) larvae as a function of release location in the BL simulation. (b) Difference in probability between the A2 and BL simulations as a function of release location. (c) Probability of settlement as a function of settlement location. (d) Difference in probability as a function of settlement location.

As noted above, the settlement rate north of 32°S was already extremely low in the BL simulation so this change can be visualized as an extension southward of the low settlement region (see Figures 8a and 8b). In contrast, settlement of vertically migrating larvae tends to increase across much of the region. Between 29.5°S and 32.5°S there is little difference in settlement rate between the simulations.

[26] Figure 8 demonstrates that there is no significant difference in seasonality or pelagic larval duration dependence between the BL and A2 simulations. That is, in the A2 simulation the tendency remains for neutrally buoyant larvae to settle only during winter, and vertically migrating larvae to settle predominantly during summer. However, the high small-scale spatial heterogeneity of the changes in probability of successful recruitment for vertically migrating larvae under A2 scenario (Figure 7b) should be noted. The regions of positive change cannot easily be associated to baseline conditions.

5. Discussion

[27] Although qualitatively similar, the coastal ocean circulation simulated for the BL and A2 scenarios contain significant quantitative differences that can have moderate to large effects on larval dispersal patterns depending on larval behavior and pelagic larval duration. The presently available evidence, both observational and from models, suggests that increased southerly winds will be a likely consequence of global warming [*Falvey and Garreaud*, 2009; *Echevin et al.*, 2011]. This tendency is present in the PRECIS A2 wind field used to force the model, in that southerly coastal winds are on average over 1 m s^{-1} stronger, and intense coastal upwelling

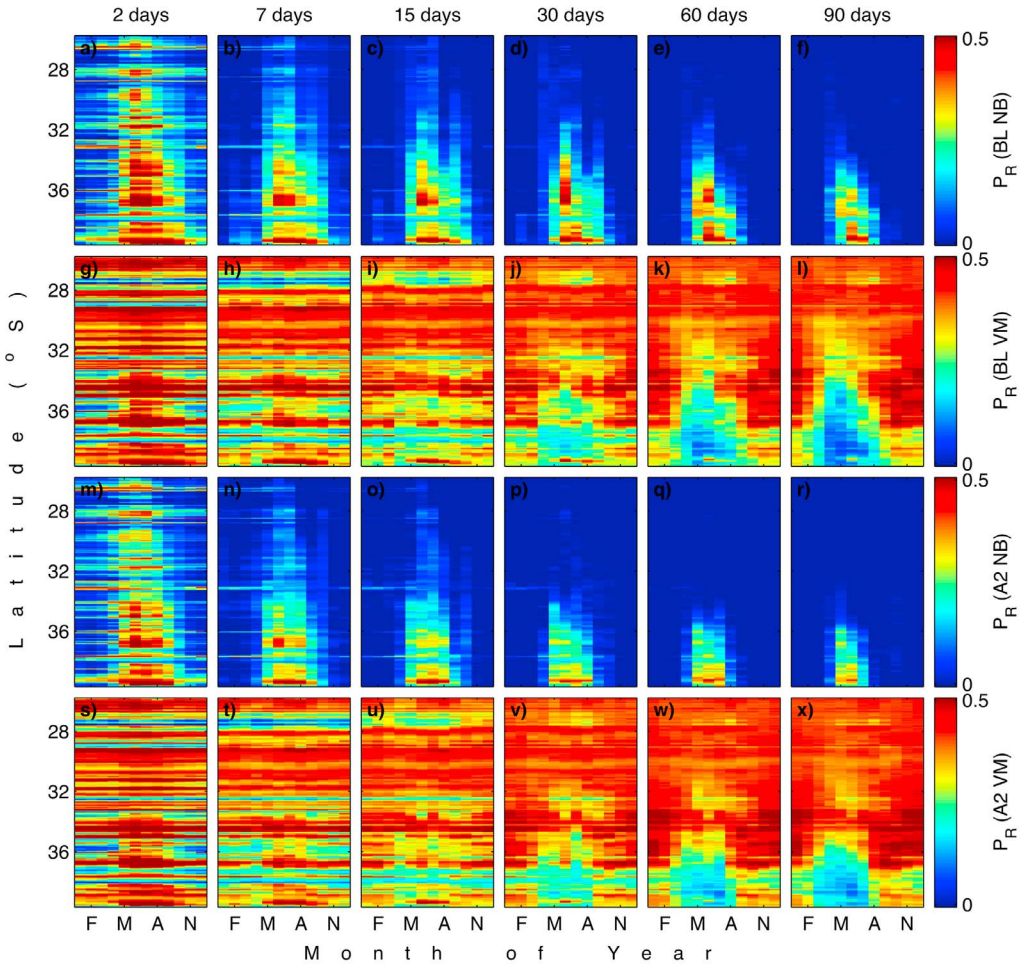

Figure 8. Monthly mean probability of settlement (P_R) as a function of pelagic larval duration (indicated at the top), month of year, release location, and swimming behavior for the BL and A2 simulations.

events over 10% more frequent, than in the BL simulation (GF). The effect of this change to the wind field upon the local ocean circulation was to intensify the upwelling circulation, evidenced by (1) stronger vertical velocities at the coast, (2) offshore advection in the surface Ekman layer and onshore transport beneath, and (3) swifter along-slope velocities, both at the surface as the upwelling jet, and underneath as the opposing poleward undercurrent. This increased coastal upwelling resulted in an annual mean reduction of SST of approximately 1°C across much of the domain and an intensification of the mesoscale eddy field. Although an increased frequency and intensity of upwelling occurs throughout the year in the A2 wind field, the reduced vertical temperature gradient in winter due to deepening of the oceanic mixed layer meant that significant surface cooling was seen only during summer. The relative cooling at the surface occurred south of 30°S, coincident with the zone of increased summer upwelling frequency shown in Figure 2.

[28] An intensification of the coastal jet and poleward undercurrent, relative to the BL simulation, was generated in the A2 simulation. A similar intensification of the Peru Undercurrent is also commonly present in several GCMs simulations, such as the GFDL CM2, under the A2 and most other emissions scenarios. The fact that a stronger Peru Undercurrent has been simulated in this and other significantly different models provides some evidence that it may be a real response of the system to altered wind forcing. While the processes driving the Peru Undercurrent are not fully understood, it is likely that the increased meridional gradient in wind stress, and hence in offshore Ekman transport, is responsible for the Peru Undercurrent intensification seen in the various models.

[29] An important result arising from this study is that the A2 intensification of the meridional current system (equatorward coastal jet plus poleward undercurrent) results in substantial changes in alongshore connectivity (Figures 6 and 7). The annual mean probability of settlement is observed to decrease for neutrally buoyant larvae as a result of the intensification of the offshore transport in the surface Ekman layer. However, for vertically migrating larvae, the settlement probability increases, particularly for latitudes south of about 32°S. Figure 8 shows that this increase is indeed greatest in the southern latitudes and during the summer months, for all values of pelagic larval duration up to 90 days. The interpretation is that the very energetic meridional (along-slope) flow results in a higher nearshore retention rate. Figures 3g and 3k indeed show that the intensified along-slope currents are accompanied by a trend toward

subsurface and near-surface convergence, which enhances vertical exchange and decreases offshore larvae loss.

[30] The upwelling favorable conditions that prevail along the central Chilean coast, especially north of about 32°S, are characterized by a near constant offshore Ekman transport of surface waters that hampers the recruitment of passive larvae released at the coast [*Strub et al.*, 1998; *Thomas*, 1999; *Navarrete et al.*, 2005]. As a result, it is likely that the larvae of persistent coastal populations possess behavioral strategies that increase their chances of returning to a suitable habitat on the shore [*Shanks*, 1995; *Queiroga et al.*, 2007; *Morgan et al.*, 2009]. Here we consider one active swimming strategy, that of diel vertical migration, wherein the larvae varies its position in the water column in a daily cycle [*Garland et al.*, 2002; *Poulin et al.*, 2002; *Queiroga et al.*, 2007]. Our results confirm that the probability of neutrally buoyant larvae being found close to shore is very low for pelagic larval durations beyond a few days. While it is probable that the intrinsic mesoscale variability in central Chile, resulting from baroclinic instability of the water upwelled at the coast, will provide pathways for larvae to return to shore, the results suggest that this mechanism for recruitment is not effective, at least in the absence of other cross-shore transport processes (e.g., internal waves, sea breeze, topographic eddies, etc). As the resolution of the ocean simulations was sufficiently high to reproduce mesoscale variability well, the low rate of settlement of neutrally buoyant larvae suggests that mesoscale structures may be ineffective at transporting larvae to shore. Nonetheless, it should be recalled that a low level of settlement success may still be sufficient to sustain a viable population, and species with neutrally buoyant larvae may compensate increased levels of larval waste through increased larval production.

[31] Our results suggest that vertically migrating larvae may have a rate of successful settlement in central Chile that is many times greater than those with neutrally buoyant larvae, at least when the vertically migrations are sufficiently deep. By sinking out of the ≈20 m thick surface Ekman layer and into the generally onshore flow beneath, vertically migrating larvae avoid offshore transport and are thus much more likely to remain near to shore [*Poulin et al.*, 2002; *Queiroga et al.*, 2007]. The fact that the water mass typically found on the Chilean shelf after upwelling is Equatorial Subsurface Water, characteristic of the core of the Peru Undercurrent [*Strub et al.*, 1998], implies that an ability to be entrained in the Peru Undercurrent is a successful larval strategy in order to return to shore. In other words, larvae that are entrained in the Peru Undercurrent would be expected to have greater chance of returning to shore. For pelagic larval durations beyond a few days, the mean displacement of both neutrally buoyant and vertically migrating larvae that successfully settled was toward the south, consistent with advection in the Peru Undercurrent. The mean displacement of unsuccessful neutrally buoyant larvae, however, was northward, reflecting the fact that offshore transport in the surface Ekman layer greatly reduces the chances of neutrally buoyant larvae returning to shore.

[32] The tight dependence of settlement probability upon upwelling intensity is reflected in its seasonality, which closely follows that of the wind field (Figure 8). Settlement of neutrally buoyant larvae occurs during winter, when offshore Ekman transport is least prevalent, and is most successful toward the south of the domain where upwelling events are less frequent. Vertically migrating larvae, however, experience greatest success in summer; it is during this season when the vertical cell is most intense (with enhanced horizontal convergence at surface and subsurface layers, Figure 3g) and the along-slope surface upwelling jet and subsurface undercurrent reach maximum values (Figure 3k). Thus, whereas for neutrally buoyant larvae the effect of upwelling is negative, for vertically migrating larvae it tends to be positive. As a result, the intensification of the upwelling circulation in the A2 scenario resulted in opposite effects on settlement of these two types of larval behaviors: lower settlement of neutrally buoyant larvae, and slightly increased settlement of vertically migrating larvae.

[33] The marked winter maximum in settlement of neutrally buoyant larvae at all release times reflects the strong dependence of settlement on the intensity of the upwelling circulation. During winter, offshore Ekman transport is weaker, and increasingly so with distance toward the south. On short larval durations the success rate is strongly biased toward winter for certain release locations south of 33°S. This may be due to the fact that larvae are released at the surface and so are initially carried offshore during the summer upwelling season. As a result, species that release their larvae below the surface Ekman layer would be expected to exhibit great larval settlement rates over short pelagic larval durations. For larval durations longer than 30 days, however, a marked minimum exists for larvae released during Autumn throughout the same region, indicating that upwelling circulation favors the settlement of vertical migrators in this region. Of course, seasonal patterns of settlement in real organisms will be strongly or completely modified by the timing of reproduction of adults and larval hatching.

[34] In addition to the general large-scale trends outlined above, the results indicate that substantial spatial variability exists in larval settlement success rate over relatively small spatial scales. The high variability is most noticeable at short pelagic larval durations for both larval swimming behaviors. In Figure 8, extremely high and extremely low export success can be seen to occur in adjacent locations for pelagic larval durations up to 7 days. While the exact pattern of settlement at short spatial scales should be treated with caution, given the fact that advection distances are comparable to the model resolution on such short time scales, nonetheless the model indicates that a realistic velocity field can sustain high geographical variability in settlement success.

6. Conclusions and Implications

[35] An intensification and poleward migration of the prevailing equatorward wind regime of the south east Pacific is a robust result in coupled GCMs forced under a range of emission scenarios that is also supported by recent observations in southern California [*García-Reyes and Largier*, 2010] and Chile [*Falvey and Garreaud*, 2009]. Our results suggest that the consequences of this atmospheric change for the Chilean coastal ocean are an intensification of the upwelling circulation, evidenced by stronger offshore Ekman transport and return flow beneath, an increase in the strength of the coastal upwelling jet and the Peru Undercurrent, and a relatively broad surface cooling of on average 1°C, most apparent during summer, and corresponding increase in

mesoscale variability. These results are consistent with other numerical [*Echevin et al.*, 2011] and observational [*Gutiérrez et al.*, 2011] studies in this region.

[36] The Chile-Peru current system is a site of intense atmosphere-ocean carbon fluxes because of the extremely high primary productivity and regular upwelling that allows the ventilation of subthermocline waters. The projected intensification of upwelling is likely to increase these fluxes because of both the biological and physical pumps. The biological pump would act within the band of nearshore upwelled waters: a scenario of increased winds would lead to enhanced vertical circulation, more nutrient supply to surface waters, increased primary productivity and enhanced removal of the near sea surface atmospheric carbon. The physical pump, on the other hand, would arise becuase of the enhanced along-slope circulation, the dominant factor being the enhanced coastal upwelling jet which brings cold waters toward lower latitudes which are then capable of releasing carbon to the atmosphere. The projected intensification of upwelling is likely to modify both these pumps, with opposing effects, representing a complex feedback on the climate system.

[37] The altered advective environment as simulated in the model has consequences for the connectivity of communities of marine organisms that populate the coast. Purely passive larvae are substantially less likely to remain close to shore under the simulated future circulation, with the result that marginally viable populations may be pushed to local extinction in the future. On the other hand, species with larvae that possess an ability to vary their position in the water column may be benefited by the future conditions, as the increased intensity and geographical and temporal scope of the upwelling circulation cell acts to increase their coastal retention. While swimming behavior, or general information about diel vertical migration, of the larvae of species that inhabit the central Chilean coastal waters is largely unknown (but see *Poulin et al.* [2002]), it is apparent that an ability to sink out of the surface Ekman layer afforded to vertically migrating species dramatically increases their chances of successful settlement, especially for pelagic larval durations longer than a few days. Empirical observations by *Poulin et al.* [2002] in central Chile with one species of benthic mollusk with long (>80 days) pelagic larval durations, which apparently undergoes diel vertical migration, support these general model results. As a result, it may be expected that the composition of coastal communities that inhabit the central Chilean coast may experience changes in the future because of an altered coastal ocean circulation alone.

[38] While relative coastal cooling along the west coast of South America is commonly produced in simulations using coupled GCMs, the oceanic components of these models are generally too coarse to recreate well the upwelling circulation and hence tend to underestimate the relative decrease in SST. Here we have shown that the relative temperature decrease may be up to 1°C in the annual average, and up to 2°C during summer. This cooling is substantially more intense than estimated by GF from a simple linear regression of historical SST and meridional wind data over the upwelling season. Considering projections of mean ocean surface warming of 1°C in the south east Pacific over the coming century [*Meehl et al.*, 2007], the net change in the temperature of coastal waters in central Chile is likely to be relatively small and may even be slightly negative. As larval development rates are commonly strongly temperature dependent, it has been hypothesized that global warming could lead to more rapid larval development and hence a lessened effective dispersal [*O'Connor et al.*, 2007; *Lett et al.*, 2010]. In this case, however, the probable weak temperature change in coastal waters means that larval durations are likely to be less affected in this way. The relative ocean surface cooling would also be expected to moderate terrestrial temperature increases, meaning that global warming in coastal areas would be expected to be substantially below the global mean, and even produce a localized cooling [*Falvey and Garreaud*, 2009]. Although these propositions need further research, one can speculate that such changes may benefit intertidal species for whom increased atmospheric temperatures would signify increased stress because of desiccation, although any advantage may be offset by increased wind speeds.

[39] **Acknowledgments.** Support for this study was provided through the Laboratorio Internacional en Cambio Global (LINCGlobal) and CMA through Fondecyt grant 1100646. We thank Rene Garreaud from the Universidad de Chile for providing the output from the PRECIS model simulations and for his useful comments. The authors thankfully acknowledge the computer resources, technical expertise, and assistance provided by the Barcelona Supercomputing Center. S.A.N. acknowledges support by FONDAP-FONDECYT grant 15001–0001 to CASEB. The comments of two anonymous reviewers greatly helped improve the manuscript.

References

Aiken, C. M., S. A. Navarrete, M. I. Castillo, and J.-C. Castilla (2007), Along-shore larval dispersal kernels in a numerical ocean model of the central Chilean coast, *Mar. Ecol. Prog. Ser.*, *339*, 13–24.

Aiken, C. M., M. I. Castillo, and S. A. Navarrete (2008), A simulation of the Chilean Coastal Current and associated topographic upwelling near Valparaíso, Chile, *Cont. Shelf Res.*, *28*, 2371–2381.

Antonov, J., Levitus, S., T. P. Boyer, M. Conkright, T. O'Brien, and C. Stephens (1998), *World Ocean Atlas 1998*, vol. 1, *Temperature of the Atlantic Ocean, NOAA Atlas NESDIS*, vol. 27, 166 pp., NOAA, Silver Spring, Md.

Atkinson, L. P., A. Valle-Levinson, D. Figueroa, R. De Pol-Holz, V. A. Gallardo, W. Schneider, J. L. Blanco, and M. Schmidt (2002), Oceanographic observations in Chilean coastal waters between Validivia and Concepción, *J. Geophys. Res.*, *107*(C7), 3081, doi:10.1029/2001JC000991.

Bakun, A. (1990), Global climate change and intensification of coastal ocean upwelling, *Science*, *247*, 198–201.

Batteen, M. L., C.-P. Hu, J. L. Bacon, and C. S. Nelson (1995), A numerical study of the effects of wind forcing on the Chile Current system, *J. Oceanogr. Soc. Jpn.*, *51*, 585–614.

Blanke, B., and S. Raynaud (1997) Kinematics of the Pacific Equatorial Undercurrent: A Eulerian and Lagrangian approach from GCM results, *J. Phys. Oceanogr.*, *27*, 1038–1053.

Brochier, T., C. Lett, and P. Fréon (2010), Investigating the "northern Humboldt paradox" from model comparisons of small pelagic fish reproductive strategies in eastern boundary upwelling ecosystems, *Fish Fish.*, *12*, 94–109, doi:10.1111/j.1467-2979.2010.00385.x

Cáceres, M. (1992), Vortices y filamentos observados en imagenes de satelite frente al area de surgencia de Talcahuano, Chile central, *Invest. Pesq.*, *37*, 55–66.

Capet, X., F. Colas, P. Penven, P. Marchesiello, and J. McWilliams (2008), Eddies in eastern boundary subtropical upwelling systems, in *Ocean Modeling in an Eddying Regime*, *Geophys. Monogr. Ser.*, vol. 177, edited by M. Hecht and H. Hasumi, pp. 131–147, AGU, Washington, D. C.

Chiu, J. M. Y., H. Wang, V. Thiyagarajan, and P. Y. Qian (2008), Different timings of larval starvation caused different latent effects on juvenile *Crepidula onyx* through different mechanisms, *Mar. Biol.*, *154*, 91–98.

Cowen, R., C. B. Paris, and A. Srinivasan (2006), Scaling of connectivity in marine populations, *Science*, *311*, 522–527.

Cury, P., C. Roy, and V. Faure (1998), Environmental constraints and pelagic fisheries in upwelling areas: The Peruvian puzzle, *S. Afr. J. Mar. Sci.*, *19*, 159–167.

Djurfeldt, L. (1989), Circulation and mixing in a coastal upwelling embayment: Gulf of Arauco, Chile, *Cont. Shelf Res.*, *9*, 1003–1016.

Echevin, V., K. Goubanova, A. Belmadani, and B. Dewitte (2011), Sensitivity of the Humboldt Current system to global warming: A downscaling experiment of the IPSL-CM4 model, *Clim. Dyn.*, *36*, 1365–1378, doi:10.1007/s00382-011-1085-2.

Estrade, P., P. Marchesiello, A. Colin De Verdière, and C. Roy (2008), Cross-shelf structure of coastal upwelling: A two-dimensional extension of Ekman's theory and a mechanism for inner shelf upwelling shut down, *J. Mar. Res.*, *66*, 589–616.

Falvey, M., and R. D. Garreaud (2009), Regional cooling in a warming world: Recent temperature trends in the southeast Pacific and along the west coast of subtropical South America (1979–2006), *J. Geophys. Res.*, *114*, D04102, doi:10.1029/2008JD010519.

Figueroa, D., and C. Moffat (2000), On the influence of topography in the induction of coastal upwelling along the Chilean coast, *Geophys. Res. Lett.*, *27*, 3905–3908.

Fuenzalida H., P. Aceituno, M. Falvey, R. Garreaud, M. Rojas, and R. Sanchez (2007), Study on climate variability for Chile during the 21st century [in Spanish], technical report, Natl. Environ. Comm., Santiago. [Available at http://www.dgf.uchile.cl/PRECIS.]

Galindo, H. M., D. B. Olson, and S. R. Palumbi (2006), Seascape genetics: A coupled oceanographic-genetic model predicts population structure of Caribbean corals, *Curr. Biol.*, *16*(16), 1622–1626.

García-Reyes, M., and J. Largier (2010), Observations of increased wind-driven coastal upwelling off central California, *J. Geophys. Res.*, *115*, C04011, doi:10.1029/2009JC005576.

Garland E. D., C. A. Zimmer, and S. J. Lentz (2002), Larval distributions in inner-shelf waters: The roles of wind-driven cross-shelf currents and diel vertical migrations, *Limnol. Oceanogr.*, *47*, 803–817.

Garreaud, R., and M. Falvey (2008), The coastal winds off western subtropical South America in future climate scenarios, *Int. J. Climatol.*, *29*, 543–554, doi:10.1002/joc.1716.

Gilg, M. R., and T. J. Hilbish (2000), The relationship between allele frequency and tidal height in a mussel hybrid zone: A test of the differential settlement hypothesis, *Mar. Biol.*, *137*, 371–378.

Gutiérrez, D., et al. (2011), Coastal cooling and increased productivity in the main upwelling zone off Peru since the mid-twentieth century, *Geophys. Res. Lett.*, *38*, L07603, doi:10.1029/2010GL046324.

Haidvogel, D. B., and A. Beckmann (1999), *Numerical Ocean Circulation Modeling*, Imp. Coll. Press, London.

Hohenlohe, P. A. (2004), Limits to gene flow in marine animals with planktonic larvae: Models of *Littorina* species around Point Conception, California, *Biol. J. Linn. Soc.*, *82*(2), 169–187.

Hormazábal, S. (1995), Caracteristicas de la circulacion oceanica y costera frente a Coquimbo, Chile (30°S), M.Sc. thesis, Univ. Catol. de Valparaiso, Valparaiso, Chile.

Hormazabal, S., G. Shaffer, and O. Leth (2004), Coastal transition zone off Chile, *J. Geophys. Res.*, *109*, C01021, doi:10.1029/2003JC001956.

Johnson, D. R., T. Fonseca, and H. Sievers (1980), Upwelling in the Humboldt Coastal Current near Valparaiso, Chile, *J. Mar. Res.*, *38*, 1–15.

Jones, R. G., M. Noguer, D. C. Hassell, D. Hudson, S. S. Wilson, G. J. Jenkins, and J. F. B. Mitchell (2004), Generating high resolution climate change scenarios using PRECIS, report, 40 pp., Met. Office Hadley Cent., Exeter, U. K.

Kistler, R., et al. (2001), The NCEP-NCAR 50-year reanalysis: Monthly means CD-ROM and documentation, *Bull. Am. Meteorol. Soc.*, *82*, 247–268

Largier, J. L. (2003), Considerations in estimating larval dispersal distances from oceanographic data, *Ecol. Appl.*, *13*, S71–S89.

Leth, O., and J. F. Middleton (2004), A mechanism for enhanced upwelling off central Chile: Eddy advection, *J. Geophys. Res.*, *109*, C12020, doi:10.1029/2003JC002129.

Leth, O., and G. Shaffer (2001), A numerical study of the seasonal variability in the circulation off central Chile, *J. Geophys. Res.*, *106*, 22,229–22,248.

Lett, C., S.-D. Ayata, M. Huret, and J. O. Irisson (2010), Biophysical modelling to investigate the effects of climate change on marine population dispersal and connectivity, *Prog. Oceanogr.*, *87*, 106–113.

Locarnini, R. A., A. V. Mishonov, J. I. Antonov, T. P. Boyer, and H. E. Garcia (2006), *World Ocean Atlas 2005*, vol. 1, *Temperature, NOAA Atlas NESDIS*, vol. 61, edited by S. Levitus, 182 pp., NOAA, Silver Spring, Md.

Longhurst, A. (1998), *Ecological Geography of the Sea*, Academic, San Diego, Calif.

Marchesiello, P., and P. Estrade (2007), Eddy activity and mixing in upwelling systems: A comparative study of northwest Africa and California regions, *Int. J. Earth Sci.*, *98*, 299–308, doi:10.1007/s00531-007-0235-6.

Marchesiello, P., J. C. McWilliams, and A. Shchepetkin (2001), Open boundary conditions for long-term integration of regional oceanic models, *Ocean Modell.*, *3*, 1–21.

Marchesiello, P., J. C. McWilliams, and A. Shchepetkin (2003), Equilibrium structure and dynamics of the California Current System, *J. Phys. Oceanogr.*, *33*, 753–783.

Mason, E., J. Molemaker, A. F. Shchepetkin, F. Colas, J. C. McWilliams, and P. Sangrà (2010), Procedures for offline grid nesting in regional ocean models, *Ocean Modell.*, *35*, 1–15, doi:10.1016/j.ocemod.2010.05.007.

Meehl, G. A., C. Covey, T. Delworth, M. Latif, B. McAvaney, J. F. B. Mitchell, R. J. Stouffer, and K. E. Taylor (2007), The WCRP CMIP3 multimodel dataset: A new era in climate change research, *Bull. Am. Meteorol. Soc.*, *88*, 1383–1394, doi:10.1175/BAMS-88-9-1383.

Mendelssohn, R., and F. B. Schwing (2002), Common and uncommon trends in SST and wind stress in California and Peru-Chile current systems, *Prog. Oceanogr.*, *53*, 141–162.

Mesias, J. M., R. P. Matano, and P. T. Strub (2001), A numerical study of the upwelling circulation off central Chile, *J. Geophys. Res.*, *106*, 19,611–19,623.

Mesias, J. M., R. P. Matano, and P. T. Strub (2003), Dynamical analysis of the upwelling circulation off central Chile, *J. Geophys. Res.*, *108*(C3), 3085, doi:10.1029/2001JC001135.

Morgan, S. G. (1995), Life and death in the plankton: Larval mortality and adaptation, in *Ecology of Marine Invertebrate Larvae*, edited by L. McEdward, pp. 279–321, CRC Press, Boca Raton, Fla.

Morgan, S. G., J. L. Fisher, S. H. Miller, S. T. McAfee, and J. L. Largier (2009), Nearshore larval retention in a region of strong upwelling and recruitment limitation, *Ecology*, *90*, 3489–3502.

Muñoz, R., and R. Garreaud (2005), Dynamics of the low-level jet off the subtropical west coast of South America, *Mon. Weather Rev.*, *133*, 3661–3677.

Narváez, D. A., S. A. Navarrete, J. Largier, and C. A. Vargas (2006), Onshore advection of warm water and larval invertebrate settlement during relaxation of upwelling off central Chile, *Mar. Ecol. Prog. Ser.*, *309*, 159–173.

Navarrete, S. A., E. Wieters, B. Broitman, and J. C. Castilla (2005), Scales of benthic-pelagic coupling and the intensity of species interactions: From recruitment limitation to top down control, *Proc. Natl. Acad. Sci. U. S. A.*, *102*, 18,046–18,051.

NOAA (2006), 2 min Gridded Global Relief Data (ETOPO2v2), http://www.ngdc.noaa.gov/mgg/fliers/06mgg01.html, Natl. Geophys. Data Cent., Boulder, Colo.

O'Connor, M., J. F. Bruno, S. D. Gaines, B. S. Halpern, S. E. Lester, B. P. Kinlan, and J. M. Weiss (2007), Temperature control of larval dispersal and the implications for marine ecology, evolution, and conservation, *Proc. Natl. Acad. Sci. U. S. A*, *104*, 1266–1271.

Poulin, E., A. T. Palma, G. Leiva, D. Narvaez, C. Pacheco, S. A. Navarrete, and J.-C. Castilla (2002), Avoiding offshore transport during upwelling events: The case of competent larvae of the gastropod *Concholepas concholepas*, *Limnol. Oceanogr.*, *47*, 1248–1255.

Queiroga H., T. Cruz, A. dos Santos, J. Dubert, J. I. González-Gordillo, J. Paula, A. Peliz, and A. M. P. Santos (2007), Oceanographic and behavioural processes affecting invertebrate larval dispersal and supply in the western Iberia upwelling ecosystem, *Prog. Oceanogr.*, *74*, 174–191, doi:10.1016/j.pocean.2007.04.007.

Rayner, N. A., D. E. Parker, E. B. Horton, C. K. Folland, L. V. Alexander, D. P. Rowell, E. C. Kent, and A. Kaplan (2003), Global analyses of sea surface temperature, sea ice, and night marine air temperature since the late nineteenth century, *J. Geophys. Res.*, *108*(D14), 4407, doi:10.1029/2002JD002670.

Sen Gupta, A., A. Santoso, A. S. Taschetto, C. C. Ummenhofer, J. Trevena, and M. H. England (2009), Projected changes to the Southern Hemisphere ocean and sea-ice in the IPCC AR4 climate models, *J. Clim.*, *22*, 3047–3078.

Shaffer, G., S. Hormazabal, O. Pizarro, and S. Salinas (1999), Seasonal and interannual variability of currents and temperature off central Chile, *J. Geophys. Res.*, *104*, 29,951–29,961.

Shanks, A. L. (1995), Mechanisms of cross-shelf dispersal of larval invertebrates and fish, in *Ecology of Marine Invertebrate Larvae*, edited by L. R. McEdward, pp. 323–368, CRC Press, Boca Raton, Fla.

Shanks, A. L., S. G. Morgan, J. MacMahan, and A. Reniers (2010), Surf zone physical and morphological regime as determinants of temporal and spatial variation in larval recruitment, *J. Exp. Mar. Biol. Ecol.*, *392*, 140–150.

Shchepetkin, A. F., and J. C. McWilliams (2005), The regional oceanic modeling system (ROMS): A split-explicit, free-surface, topography-following-coordinate oceanic model, *Ocean Modell.*, *9*, 347–404.

Strub, P. T., J. M. Mesias, and C. James (1995), Altimeter observations of the Peru-Chile Countercurrent, *Geophys. Res. Lett.*, *22*, 211–214.

Strub, P. T., J. M. Mesias, V. Montecino, J. Rutllant, and S. Salinas (1998), Coastal ocean circulation off western south America, in *The Sea*, vol. 11, *The Global Coastal Ocean: Regional Studies and Syntheses*, edited by A. R. Robinson and K. H. Brink, pp. 273–313, John Wiley, Hoboken, N. J.

Thomas, A. C. (1999), Seasonal distributions of satellite-measured phytoplankton pigment concentration along the Chilean coast, *J. Geophys. Res.*, *104*, 25,877–25,890.

Vargas, C. A., P. H. Manríquez, and S. A. Navarrete (2006), Feeding by larvae of intertidal invertebrates: Assessing their position in pelagic food webs, *Ecology*, *87*, 444–457.

C. M. Aiken and S. A. Navarrete, Estación Costera de Investigaciones Marinas, Pontificia Universidad Católica de Chile, Osvaldo Marin 1672, Las Cruces, Chile. (cm.aiken@yahoo.com; snavarrete@bio.puc.cl)

J. L. Pelegrí, Departament d'Oceanografia Física, Institut de Ciències del Mar, CMIMA, CSIC, Passeig Maritim de la Barceloneta 37-49, E-08003 Barcelona, Spain. (pelegri@icm.csic.es)